

Conformations and dynamics of adsorbed protein-like chains

Tingting Sun^{a,b}, Linxi Zhang^{a,*}

^aDepartment of Physics, Wenzhou Normal College, Wenzhou 325027, People's Republic of China

^bDepartment of Physics, Zhejiang University, Hangzhou 310027, People's Republic of China

Received 16 February 2005; received in revised form 20 April 2005; accepted 12 May 2005

Available online 9 June 2005

Abstract

Conformations and dynamics of adsorbed protein-like chains are investigated by using Monte Carlo simulation based on the modified orientation-dependent monomer–monomer interaction (ODI) model. The chain size and shape of adsorbed protein-like chains, such as mean-square end-to-end distance $\langle R^2 \rangle$, mean-square radius of gyration $\langle S^2 \rangle_{xy}$ (or $\langle S^2 \rangle_z$), shape factors $\langle sf_i^* \rangle$ ($i = 1, 2, 3$), and $\langle \delta^* \rangle$ are discussed here. At the same time, fraction of adsorbed segment f_a and average orientation of bond $\langle P_2(\cos \theta) \rangle$ are also investigated. The adsorbed protein-like chains trend to be more flat when adsorption interaction energy becomes strong. Different kinds of interactions (such as contact interaction, sheet interaction, spin–spin interaction, helical interaction, and adsorbed interaction) are considered in detail. Dynamics of adsorbed protein-like chains are investigated by calculating their diffusion coefficients, and we find that there exist the relationships of $D_{xy} \sim N^{-\gamma_{xy}}$ and $D_z \sim N^{-\gamma_z}$, and the values of γ_{xy} and γ_z are 4–5 times larger than that of general self-avoiding walk (SAW) chains. These investigations may provide some insights into adsorption of proteins.

© 2005 Elsevier Ltd. All rights reserved.

Keywords: Conformation; Protein-like chain; Adsorption

1. Introduction

The adsorption of proteins at solid- and gas–liquid interfaces is receiving more attention, and it is an important and challenging interdisciplinary field of natural sciences [1–8]. In some cases, the adsorption of proteins plays a key role for both fundamental biochemical and biophysical processes and a variety of applications including biomaterials, extracorporeal therapy, drug delivery, and solid-phase diagnostic [9]. Most experimental studies of protein adsorption employ techniques that yield only a global indication of the structure of proteins [10] (physicochemical methods providing detailed information about the protein structure are also available, but the time resolution is usually not sufficient in order to study the kinetics of the rearrangement processes in detail). The relative experiment apparatus such as atomic force microscopy (AFM) has been used widely in the study of the adsorption phenomenon. The

field is also very interesting from a purely academic perspective, since it contains several non-trivial problems and poorly understood phenomena related to biological surface science and statistical physics.

Simulation of protein adsorption is still lacking, and it is connected with the theory of structural alterations (folding or denaturation) of proteins in the bulk of the solution (models developed for the bulk are immediate constituents of those for the surface). Although details of Monte Carlo simulations are just dependent on the model assumptions, Monte Carlo method is still a powerful tool to analyze polymer chains systems including the exact description of spatial correlations among adsorbed species and dynamic properties [11–15]. As protein adsorption bears some resemblance to the adsorption of polymer chains, Monte Carlo method can be used to study the protein adsorption [16–22].

Proteins are heterogeneous chain molecules composed of sequences of amino acids, therefore, protein chains have many conformations generated by rotation around bonds since bond length and angles are fairly invariant in the known protein structures, and protein conformations is very significant. At the same time, the understanding of the kinetics of protein adsorption should be recognized, and the

* Corresponding author. Tel.: +86 571 88483790; fax: +86 571 87951328.

E-mail address: lxzhang@hzcnc.com (L. Zhang).

diffusion of proteins adsorbed at solid–liquid interfaces is of considerable intrinsic interest and also important for understanding the kinetics of protein adsorption. In this paper, we investigate conformations and dynamics of adsorbed protein-like chains by using Monte Carlo simulation based on the modified orientation-dependent monomer–monomer interaction model [23], and our aim is to investigate the effect of secondary structure of protein-like chain on the adsorption of protein-like chains.

2. Model

Our simulation is mainly based on the ODI model (Orientation-Dependent Monomer–Monomer Interactions) which is presented by Zhdanov and Kasemo [23], and we have also some improvements on the model [24]. In our modified ODI model, α -helical and β -sheet structures can be taken into account simultaneously. Therefore, our model can be more close to the real protein. However, this model is also lattice approximation, and that is: a protein-like chain is schematically viewed as a linear sequence of $N+1$ monomers, and the protein-like chains are constrained to be nearest-neighbors on the three-dimensional cubic lattice (each lattice site can only be occupied by one monomer). In this model, the energy of adsorbed protein-like chain is assumed to contain five terms, i.e.

$$E = \sum_{|i-j|\geq 3} \varepsilon_{ij}^{is} \delta(r_{ij} - a) + \sum_{|i-j|\geq 3} \varepsilon_{ij}^{ss} \delta(r_{ij} - a) + \sum_{i=1}^{N-1} A(\vec{s}_i \vec{s}_j) + \varepsilon_{hel} n_{hel} + \varepsilon_{ads} n_{ads} \quad (1)$$

where r_{ij} is the distance between monomers i and j , and a is the lattice spacing (in fact, $a=1$ in our calculation). Here $\delta(x)=1$ for $x=0$, and $\delta(x)=0$ for $x\neq 0$. The unit vector \vec{s}_i represents the orientation of monomer, and $(\vec{s}_i \vec{s}_j)$ is a scalar product of the orientation vectors. ε_{ij}^{is} is the isotropic (e.g. van der Waals) monomer–monomer interaction, so the first term of Eq. (1) represents the contact energy. ε_{ij}^{ss} corresponds to the hydrogen bonds in topological contacts. Bearing in mind the conditions necessarily for formation of hydrogen bonds, we consider that the values of ε_{ij}^{ss} is negative if (i) one of the monomers is directed toward the other monomer (e.g. $\vec{r}_i + \vec{s}_i = \vec{r}_j$), and (ii) simultaneously the vectors \vec{s}_i and \vec{s}_j are parallel. In all the other cases, $\varepsilon_{ij}^{ss} = 0$. In fact, we consider the second term of Eq. (1) to be β -sheet energy. The third term (with $A > 0$), constructed in analogy with the Ising antiferromagnetic spin–spin interaction, describes the orientational dependence of the interaction between nearest-neighbor monomers linked via the peptide bonds. Its goal is to reproduce an antiparallel orientation of nearest-neighbor monomers. In the fourth term of Eq. (1), ε_{hel} is the energy of one helix, and n_{hel} is the number of helix, therefore, $\varepsilon_{hel} n_{hel}$ represents the total

energy of α -helical structures. The last term is the adsorption energy of protein-like chains. If one monomer is adsorbed on the surface, the energy is entitled to ε_{ads} . Thus total adsorption energy of protein-like chain with n_{ads} adsorbed monomers is $\varepsilon_{ads} n_{ads}$.

In our simulation, we use $\varepsilon^{is} = -3.0$, $\varepsilon^{ss} = -1.5$, $A = 0.5$ and $\varepsilon_{hel} = -1.5$ [23,24] (in units of $k_B T$). In the meantime, the value of ε_{ads} is 0, -3 , -6 , and -9 (in units of $k_B T$), respectively. Different interactions between protein-like chains and the surface can lead to have different results in the conformations and dynamics of adsorbed protein-like chains.

In order to study conformations and dynamics of adsorbed protein-like chains, we have employed the classical Monte Carlo sampling algorithm, and the standard algorithm for end, corner, and crankshaft monomer moves have been used [25,26]. First the monomer chain is produced at random in the three-dimensional lattice considering the exclude volume, and the orientations of monomers are chosen at random among the allowed orientations. Then a monomer is chosen at random. If it is an end monomer, one of the neighboring lattice sites is also selected at random for an end move. If it is not an end monomer, then it can do either a corner move or a crankshaft move depending on the position of its neighbors along the chain. The possible direction of the latter move is selected at random. The trial will end if the move selected violates the excluded volume constraint by moving the monomer to an occupied site. If there is no such constraint, the energies of the original and new conformations are calculated. And the Metropolis sampling algorithm is adopted: if $E_{new} - E_{old} < 0$, the new conformation of the chain is an ‘important’ state which is accepted; and if $E_{new} - E_{old} > 0$, the new conformation of the chain is not discarded simply, otherwise the thermal movement would be ignored. A random number ζ within the range (0, 1) is produced because here Boltzmann factor $\gamma = \exp[-(E_{new} - E_{old})/k_B T]$ is always less than 1. If γ is greater than or equal to ζ the new conformation of the chain is fairly an ‘important’ state which is accepted. Only when γ is less than ζ , the new conformation of the chain is rejected and the old conformation is still kept. After each attempt of an elementary monomer move, we execute one attempt to change the orientation of the moved monomer without changing the monomer positions (also by using the Metropolis rule).

Here we use some parameters to describe the chain shape of protein-like chain. Besides of mean-square end-to-end distance $\langle R^2 \rangle$ and mean-square radius of gyration $\langle S^2 \rangle_{xy}$ (or $\langle S^2 \rangle_z$), we also explore shape factors $\langle sf_i^* \rangle$ and asphericity factor $\langle \delta^* \rangle$. The instantaneous shape of an individual configuration may be described by several ratios based on the principal components $L_1^2 \leq L_2^2 \leq L_3^2$ of $S^2 = L_1^2 + L_2^2 + L_3^2$, i.e. the orthogonal components of the squared radius of gyration taken along the principal axes of inertia [27,28]. Reducing the principal components by S^2

yields shape-factors [29], we have

$$\langle sf_i^* \rangle = \langle L_i^2 / S^2 \rangle \quad (i = 1, 2, 3) \quad (2)$$

In fact, it represents the shape of coils independent of the global size of individual configurations.

Another parameter [30,31] characteristic of the shape of molecules may be obtained by combining the reduced components of S^2 to a single quantity that varies between 0 (sphere) and 1 (rod)

$$\langle \delta^* \rangle = 1 - 3 \left\langle \frac{L_1^2 L_2^2 + L_2^2 L_3^2 + L_3^2 L_1^2}{(L_1^2 + L_2^2 + L_3^2)^2} \right\rangle \quad (3)$$

The parameter $\langle \delta^* \rangle$ is a useful measure of the instantaneous anisotropy or deviation from sphericity of the walk [32]. For example, for star-branched random walk chains, the numerical values of $\langle \delta^* \rangle$ are 0.3947, 0.3044, 0.2427, 0.1310, 0.0892 and 0 for $F=2, 3, 4, 8, 12, \infty$ [31,33]. It shows that when $F=\infty$, the configuration of molecule approaches globular, therefore, the value of $\langle \delta^* \rangle$ is 0. For linear random walk chains ($F=2$), $\langle \delta^* \rangle=0.3947$, and the shape of molecules is not a globe.

The fraction of adsorbed segments f_a is defined as:

$$f_a = \frac{N_a}{N + 1} \quad (4)$$

here N_a is the number of chain monomers adsorbed on the surface, and N is chain length of adsorbed protein-like chains.

The orientation of the chain segments can be monitored by the angles θ between the z -axis and the bonds. A convenient quantity to distinguish the directions of the bonds is

$$\langle P_2(\cos \theta) \rangle \equiv \left\langle \frac{1}{2}(3 \cos^2 \theta - 1) \right\rangle \quad (5)$$

This parameter will take $-0.5, 0$ and 1.0 for bonds that are perpendicular, randomly oriented, and parallel to z -direction respectively.

Lastly, the dynamics of adsorbed protein-like chains are investigated through calculating the center-of-mass diffusion coefficient, defined as [16,34]:

$$D = \frac{[\langle (\Delta x)^2 \rangle + \langle (\Delta y)^2 \rangle + \langle (\Delta z)^2 \rangle]}{6t} \quad (\text{for large } t) \quad (6)$$

where

$$\Delta x = \sum_i (x_i(t) - x_i(0)) / (N + 1) = (x_{c,m}(t) - x_{c,m}(0)),$$

$$\Delta y = \sum_i (y_i(t) - y_i(0)) / (N + 1)$$

$$= (y_{c,m}(t) - y_{c,m}(0)), \text{ and}$$

$$\Delta z = \sum_i (z_i(t) - z_i(0)) / (N + 1) = (z_{c,m}(t) - z_{c,m}(0))$$

t is the diffusion time measured in MCS [1 MCS is defined as a move per monomer].

3. Results and discussion

3.1. Chain size and shape

We first investigate chain size and shape of adsorbed protein-like chains with different adsorption energy ϵ_{ads} and SAW (self-avoiding walk) chains with $\epsilon_{\text{ads}} = -0$. Fig. 1 shows mean-square end-to-end distance $\langle R^2 \rangle$ as a function of chain length N for adsorbed protein-like chains and SAW chains. In the two-double logarithm scale, the plots all fit a good linear, which satisfies $\langle R^2 \rangle \sim N^{2\nu_R}$. The theoretic exponent ν_R for two-dimensional self-avoiding walk chain is 0.75, which is derived by Nienhuis [35]. In our simulation, the exponent for SAW chain with adsorbed energy $\epsilon_{\text{ads}} = -9$ is 0.70, and the value is very close to $\nu_R = 0.75$ for two-dimensional self-avoiding walk chain. In fact, three-dimensional SAW chains with very strong adsorbed energy can be just seen as a two-dimensional SAW chains. In Fig. 1, we also find that the exponent ν_R of protein-like chain without adsorbed energy is 0.29. When the adsorbed energy increases, the exponent also increases. For example, the value of exponents ν_R for $\epsilon_{\text{ads}} = -3, -6$, and -9 is 0.34, 0.61, and 0.61, respectively. Protein-like chains with very strong adsorbed interaction can be regarded as two-dimensional protein-like chains. As the exponent ν_R for two-dimensional chain is larger than that for three-dimensional chain, the exponent ν_R increases with adsorbed energy increasing. In the meantime, the exponent ν_R for protein-like chain is smaller than that for general polymer chain. The reason may be that protein-like chains have many interior interactions such as α -helical and β -sheet interactions while general polymer chains have not any interior interactions. Therefore, the structures of protein-like chains are more

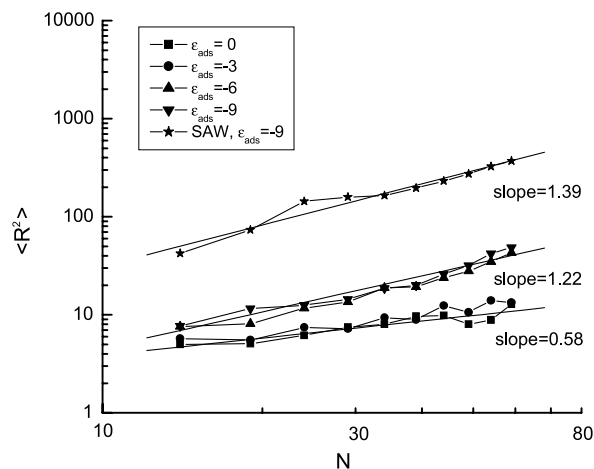


Fig. 1. Mean-square end-to-end distance $\langle R^2 \rangle$ as a function of chain length N for protein-like chains with different adsorption energy $\epsilon_{\text{ads}} = 0, -3, -6$, and -9 . Here SAW chains with $\epsilon_{\text{ads}} = -9$ are also considered.

compact, and this leads to have a small exponent ν_R in $\langle R^2 \rangle \sim N^{2\nu_R}$.

Fig. 2 shows the mean-square radii of gyration $\langle S^2 \rangle_{xy}$ and $\langle S^2 \rangle_z$ as a function of chain length N for protein-like chains with different adsorption energy and SAW chains with $\epsilon_{\text{ads}} = -9$. It is also found that $\langle S^2 \rangle_{xy} \sim N^{2\nu_{xy}}$ and $\langle S^2 \rangle_z \sim N^{2\nu_z}$, and the value of ν_{xy} is 0.33, 0.42, 0.59, and 0.65 for protein-like chains with $\epsilon_{\text{ads}} = 0, -3, -6,$ and -9 , respectively. However, the value of ν_{xy} for SAW chain with $\epsilon_{\text{ads}} = -9$ is 0.67. In the meantime, we find that the value of ν_z has a different behavior with ν_{xy} , and it decreases with adsorption interaction increasing. For example, the value of ν_z is 0.36, 0.26, 0.24, and 0.11 for protein-like chains with $\epsilon_{\text{ads}} = 0, -3, -6,$ and -9 , respectively. However, there does not exist the scaling behavior of $\langle S^2 \rangle_z \sim N^{2\nu_z}$ for SAW chains with $\epsilon_{\text{ads}} = -9$. When the adsorption energy increases, the number of adsorbed monomers also increases,

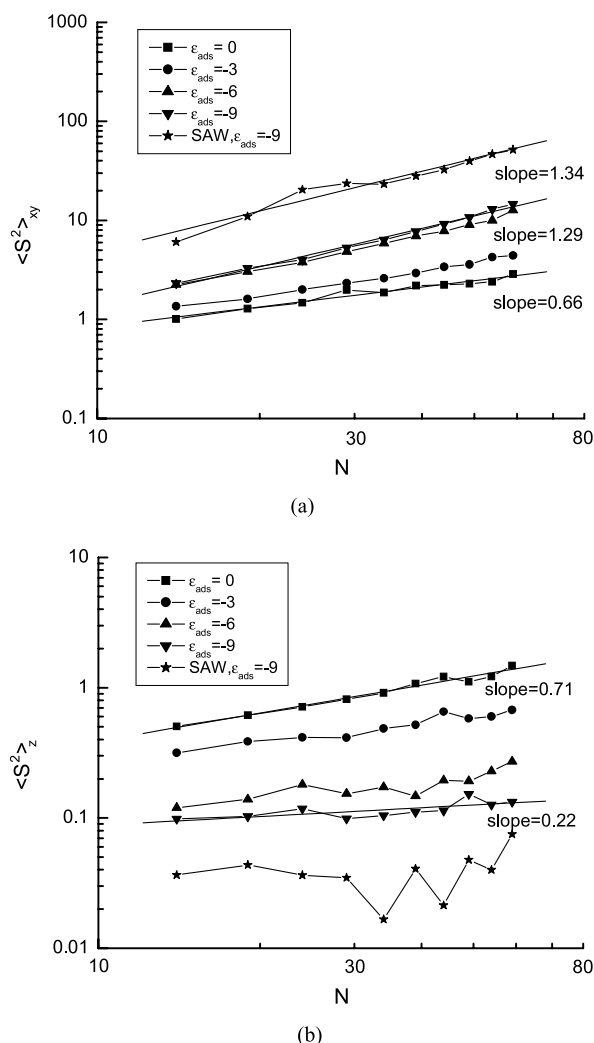


Fig. 2. Mean-square radii of gyration $\langle S^2 \rangle_{xy}$ (a) and $\langle S^2 \rangle_z$ (b) as a function of chain length N for protein-like chains with different adsorption energy $\epsilon_{\text{ads}} = 0, -3, -6,$ and -9 . Here SAW chains with $\epsilon_{\text{ads}} = -9$ are also considered.

therefore, the value of ν_{xy} increases while the value of ν_z decreases.

We then discuss the shapes of adsorbed protein-like chains through calculating $\langle sf_i^* \rangle$ ($i = 1, 2, 3$) and $\langle \delta^* \rangle$ for protein-like chains with different adsorption energy, and the results are given in Fig. 3. In Fig. 3(a), we find that the ratio of $\langle sf_1^* \rangle : \langle sf_2^* \rangle : \langle sf_3^* \rangle$ is 1:1.5: 2.5 for 60-monomer protein-like chain without adsorption interaction, and its structure is globular. While adsorption interaction becomes $\epsilon_{\text{ads}} = -9$, the ratio of $\langle sf_1^* \rangle : \langle sf_2^* \rangle : \langle sf_3^* \rangle$ becomes 1:10:40, therefore the structure is very flat. At this situation, most of monomers are adsorbed on the surface. The results for another shape parameter of $\langle \delta^* \rangle$ for protein-like chains with different adsorption interactions and SAW chain with adsorption

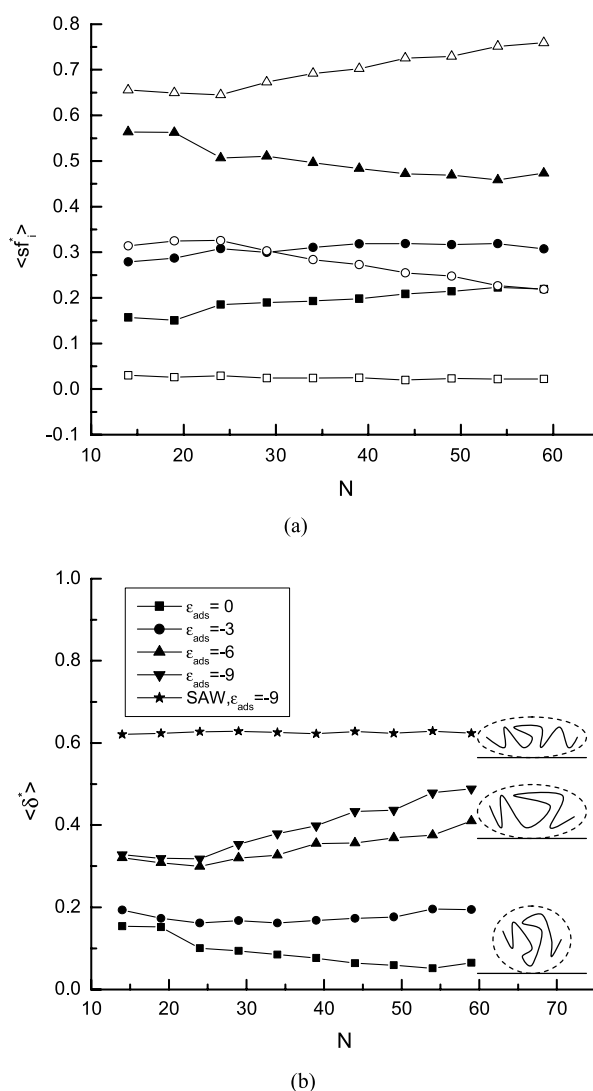


Fig. 3. Shape factor $\langle sf_i^* \rangle$ ($i = 1, 2,$ and 3) and $\langle \delta^* \rangle$ as a function of chain length N for protein-like chains. Here (a) symbols (■, □) represent protein-like chains with $\epsilon_{\text{ads}} = 0$ and -9 for $i = 1$; symbols (●, ○) represent chains with $\epsilon_{\text{ads}} = 0$ and -9 for $i = 2$; and symbols (▲, △) represent chains with $\epsilon_{\text{ads}} = 0,$ and -9 for $i = 3$ (b) protein-like chains with different adsorption energy $\epsilon_{\text{ads}} = 0, -3, -6,$ and -9 , and SAW chains with $\epsilon_{\text{ads}} = -9$ are considered.

interaction energy of $\epsilon_{\text{ads}} = -9$ are also given in Fig. 3(b). The value of $\langle \delta^* \rangle$ is 0.06, 0.19, 0.49, and 0.49 for 60-monomer chains with $\epsilon_{\text{ads}} = 0, -3, -6,$ and -9 , respectively. However, the value of $\langle \delta^* \rangle$ becomes 0.62 for SAW chain with adsorption energy of $\epsilon_{\text{ads}} = -9$. In fact, $\langle \delta^* \rangle = 0$ means that the shape of the chain is sphere, and $\langle \delta^* \rangle = 1$ shows that the shape is rod. In general, the structure of protein-like chain is globular because there exist several secondary interactions such as contact, sheet, spin–spin, and helical interactions. If it is adsorbed on a surface, the structure of proteins becomes flatter. On the other hand, the value of $\langle \delta^* \rangle$ for SAW chain with $\epsilon_{\text{ads}} = -9$ is larger than that for protein-like chain with the same adsorption energy. It is to say that the structure of SAW chain is much flatter. The reason may be that there exist complex interactions in the interior of protein-like chains.

In order to investigate the reason why there exist different statistical properties of adsorbed proteins, we here introduce the fraction of adsorbed segments f_a . Fig. 4 gives the plots of f_a as a function of chain length N , and f_a increases with adsorption energy increasing. For example, f_a is only 0.013 for protein-like chains with $\epsilon_{\text{ads}} = 0$, and it increases to 0.894 for protein-like chains with $\epsilon_{\text{ads}} = -9$. This means that 89% monomers of protein-like chains are adsorbed on the surface. We also find that f_a for SAW chains with $\epsilon_{\text{ads}} = -9$ is close to 99.7%, and all the monomers are nearly adsorbed on the surface. The reason why the fraction of adsorbed segments f_a for SAW chains with $\epsilon_{\text{ads}} = -9$ are larger than that for protein-like chains may be that there exists secondary structure in protein-like chains. Fractions of adsorbed segment $f_a(z)$ as a function of surface layer z for 40-monomer protein-like chain and 40-monomer SAW chains are shown in Fig. 5. Certainly, $f_a(z)$ at $z=0$ is the largest one for adsorbed protein-like chain, and $f_a(z)$ at $z=1$ drops sharply for protein-like chains with $\epsilon_{\text{ads}} = -6,$ and $-9,$ and SAW chain with $\epsilon_{\text{ads}} = -9$. At the large layer, f_a is

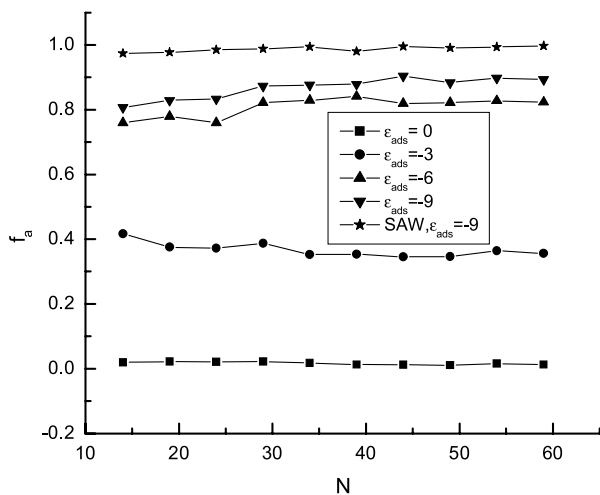


Fig. 4. Fraction of adsorbed segment f_a as a function of chain length N for protein-like chains with different adsorption energy $\epsilon_{\text{ads}} = 0, -3, -6,$ and -9 . Here SAW chains with $\epsilon_{\text{ads}} = -9$ are also considered.

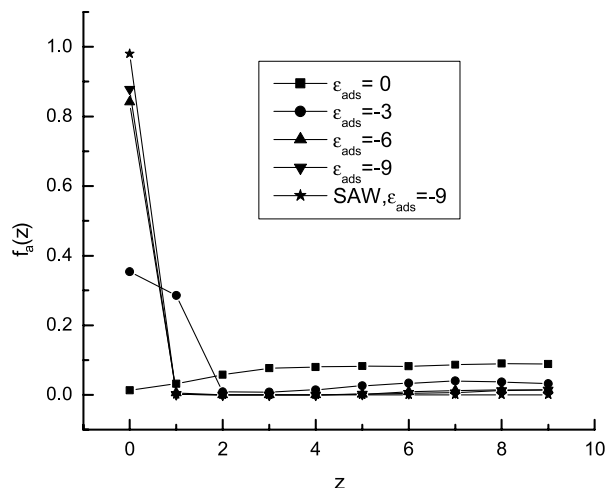


Fig. 5. Fraction of adsorbed segment $f_a(z)$ as a function of surface layer z for 40-monomer protein-like chains with different adsorption energy $\epsilon_{\text{ads}} = 0, -3, -6,$ and -9 . Here SAW chains with $\epsilon_{\text{ads}} = -9$ are also considered.

close to 0. On the other hand, $f_a(z)$ for protein-like chains with $\epsilon_{\text{ads}} = 0$ increases with z increasing.

Fig. 6 shows the average orientation of bond $\langle P_2(\cos \theta) \rangle$ on the adsorbed surface as a function of chain length N for protein-like chains and SAW chains. We find that the value of $\langle P_2(\cos \theta) \rangle$ is independent of chain length. For example, the values of $\langle P_2(\cos \theta) \rangle$ for 60-bond protein-like chains with $\epsilon_{\text{ads}} = 0,$ and -3 are -0.076 and -0.13 , respectively. As we all know that $\langle P_2(\cos \theta) \rangle = 0$ means the bonds are randomly oriented, and $\langle P_2(\cos \theta) \rangle = -0.5$ means the bonds are perpendicular to the z -direction. In our simulation, the values of $\langle P_2(\cos \theta) \rangle$ for protein-like chains with strong adsorption energy, i.e. $\epsilon_{\text{ads}} = -6,$ and -9 are -0.48 and -0.49 , respectively, and which is close to -0.5 . Therefore, the bonds of protein-like chains with strong adsorption energy are almost perpendicular to the z -direction. In the

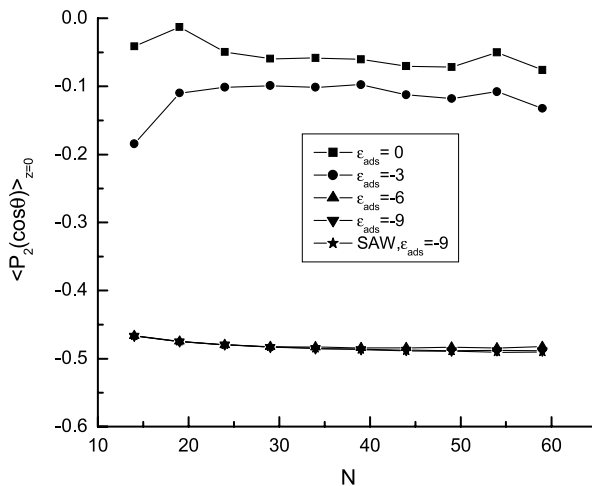


Fig. 6. Average orientation of bond $\langle P_2(\cos \theta) \rangle$ on the adsorbed surface as a function of chain length N for protein-like chains with different adsorption energy $\epsilon_{\text{ads}} = 0, -3, -6,$ and -9 . Here SAW chains with $\epsilon_{\text{ads}} = -9$ are also considered.

meantime, $\langle P_2(\cos \theta) \rangle$ for protein-like chains with $\varepsilon_{\text{ads}}=0$ is -0.05 , which is very close to zero, and the bonds are nearly randomly oriented.

3.2. Average energy

From Eq. (1), we know that the total energy can be divided into five kinds of energies: contact energy, sheet energy, spin–spin energy (reproducing an anti-parallel orientation of nearest-neighbor monomers), helical energy and adsorbed energy. The total energy and five kinds of energies as a function of chain length N for protein-like chains are shown in Fig. 7. In Fig. 7(a), the total energy per bond increases with adsorption interaction energy increasing, and decreases with chain length N increasing.

We then analyze the relationship between contact energy per bond and chain length N . In Fig. 7(b), we find that contact energy per bond decreases with adsorption interaction energy increasing. The reason may be that protein-like chains with strong adsorption interaction energy can be regarded as two-dimensional protein-like chains. Therefore, the average number of contacts for two-dimensional protein-like chain is certainly smaller than that for three-dimensional protein-like chain. The contact energy per bond for 59-bond protein-like chains with $\varepsilon_{\text{ads}}=-9$ is 57.1% smaller than that for protein-like chains without adsorption interaction energy. Another important result is that contact energy per bond decreases with chain length N increasing. In fact, the average number of contact per monomer is large for long chain. We all know that the average number of contact per monomer can be written as

$$C = \frac{1}{2} \frac{\sum_{i=1}^{N+1} \sum_{j=1}^{N+1} C_{i-j}}{N+1} \quad (7)$$

Here N is chain length, and C_{i-j} is the number of contact between i monomer and j monomer. If we suppose that the ability to form contact for each monomer is equal, i.e. $C_{i-j}=b$, we can obtain $C=(N/2)b$ from Eq. (7). Therefore, average number of contact per bond increases with chain length N increasing. That can explain why average contact energy per bond is small for large N .

Fig. 7(c) gives average sheet energy per bond as a function of chain length N , and similar results with average contact energy per bond are obtained. Average sheet energy per bond for protein-like chains with strong adsorption interaction energy is larger than that for weak adsorption energy. It shows that globular structure of protein-like chains is not only easy to form contact but also easy to form β -sheet. Average sheet energy for protein-like chains with $\varepsilon_{\text{ads}}=-9$ is about 50.0% larger than that with $\varepsilon_{\text{ads}}=0$. With chain length increasing, average sheet energy per bond drops. The explanation is similar to average contact energy per bond. If the ability to form sheet is equal for each monomer, average sheet number per bond is in proportion to chain length N , especially for weak adsorption energy.

Average spin–spin interaction energy is also discussed here. This interaction energy has relation to the anti-parallel orientation of nearest-neighbor monomers. In Fig. 7(d), average spin–spin interaction energy has a small value when adsorption energy becomes strong. However, the difference is not much obvious as the other interaction energies discussed above. There also exists the phenomenon that average spin–spin interaction energy becomes small for long chain.

Average helical energy per bond as a function of chain length is given in Fig. 7(e). We find that average helical energy per bond is almost the same for different chain length N , and it is different from Fig. 7(b)–(d). If the adsorption energy is very weak (for example $\varepsilon_{\text{ads}}=0$, or -3), average helical energy per bond is only -0.8 . However, it increases when adsorption energy becomes strong. The reason may be that helix structures exist mainly in three-dimensional globular protein. For example, average helical energy for protein-like chains with $\varepsilon_{\text{ads}}=-9$ is only -0.08 because protein-like chains with $\varepsilon_{\text{ads}}=-9$ have two-dimensional structures.

Average adsorbed energy per bond is also calculated here, and it keeps a constant value for different chain length under the condition of same adsorption energy. Average adsorbed energy per bond decreases when adsorption interaction energy becomes strong. In fact, the number of monomers adsorbed on the surface increases with the attractive interaction increasing.

3.3. Dynamics of protein-like chains

In order to investigate dynamics of protein-like chains, we first calculate the mean-square displacements of adsorbed protein-like chain. We define the mean-square displacement as

$$g_{xy}(t) = \langle (\Delta x)^2 \rangle + \langle (\Delta y)^2 \rangle \equiv \langle (x_C(t) - x_C(0))^2 \rangle + \langle (y_C(t) - y_C(0))^2 \rangle \quad (8)$$

$$g_z(t) = \langle (\Delta z)^2 \rangle \equiv \langle (z_C(t) - z_C(0))^2 \rangle \quad (9)$$

Here time is in the unit of MCS. At the same time, the diffusion coefficient D can be written as

$$D_{xy} = \frac{g_{xy}(t)}{6t} \quad (\text{for large } t) \quad (10)$$

$$D_z = \frac{g_z(t)}{6t} \quad (\text{for large } t) \quad (11)$$

Fig. 8 shows the mean-square displacement as a function of time for 30-monomer protein-like chain with $\varepsilon_{\text{ads}}=-9$. In Fig. 8, it is found that the mean-square displacements $g_{xy}(t)$ and $g_z(t)$ have a good linear with time for $t > 3 \times 10^4$ MCS, and the slopes of these two lines are 8.73×10^{-7} and 1.02×10^{-7} , respectively. Therefore, we can obtain that the values of D_{xy} and D_z are 1.455×10^{-7} and 1.7×10^{-8} , respectively.

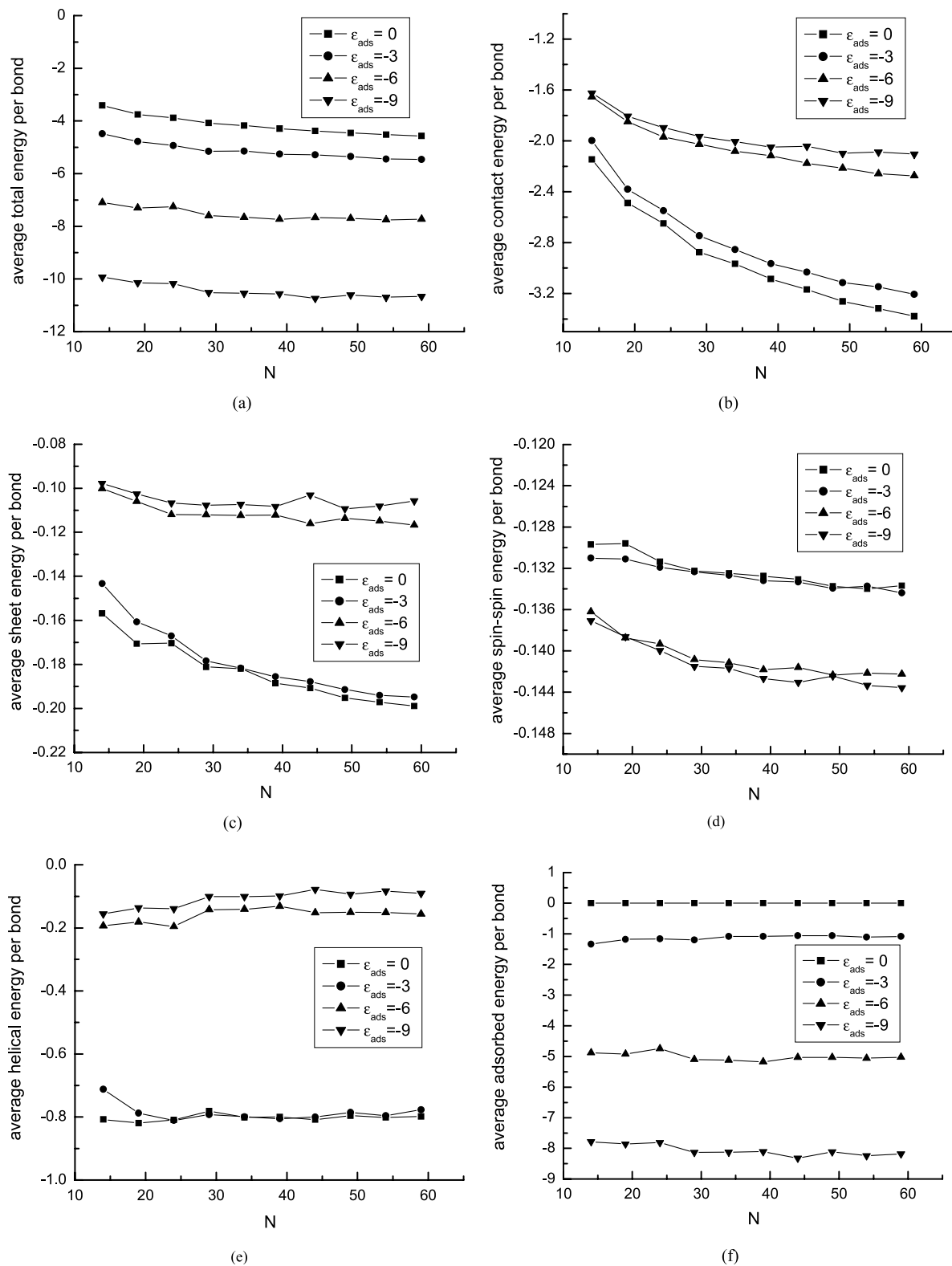


Fig. 7. Average energy per bond as a function of chain length N for protein-like chains with different adsorption energy $\epsilon_{\text{ads}}=0, -3, -6,$ and -9 . Here (a) total energy per bond, (b) contact energy per bond, (c) sheet energy per bond, (d) spin–spin energy per bond, (e) helical energy per bond, and (f) adsorbed energy per bond.

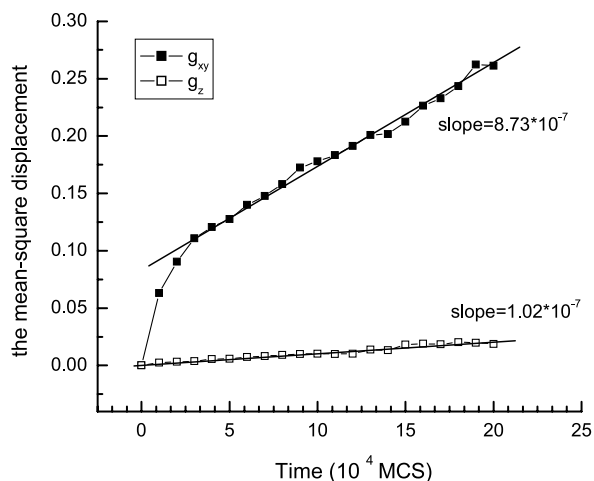


Fig. 8. The mean-square displacement as a function of time for 30-monomer protein-like chains with $\epsilon_{\text{ads}} = -9$.

Fig. 9 shows the diffusion coefficients D_{xy} and D_z as a function of $1/N$ for protein-like chains with different adsorption interaction energy. It is easily observed that in the two-double logarithm scale, there are good linear fits for these data. Therefore, there exist relationships between the diffusion coefficients and chain length N , i.e.

$$D_{xy} \sim N^{-\gamma_{xy}} \quad (12)$$

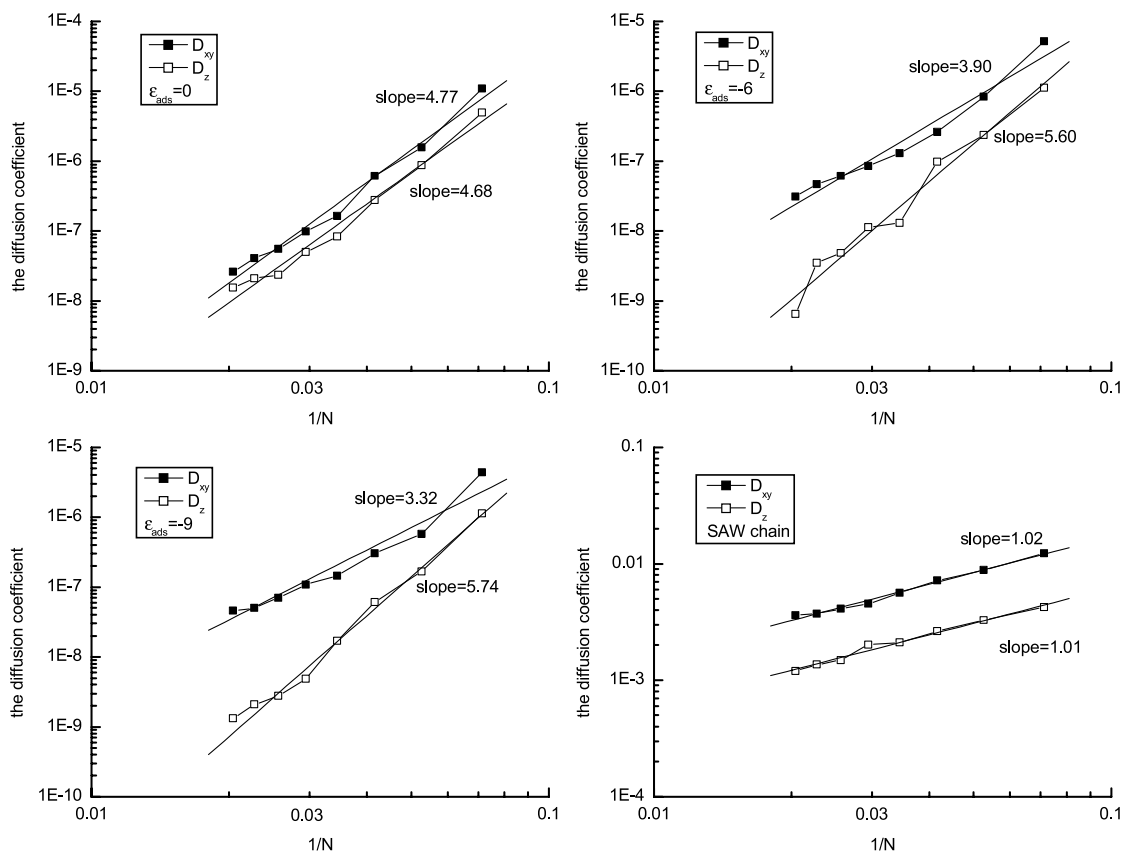


Fig. 9. The diffusion coefficient as a function of $1/N$ for protein-like chains with different adsorption energy $\epsilon_{\text{ads}} = 0, -3, -6, \text{ and } -9$. Here general SAW chains without adsorption are considered, and N is chain length.

$$D_z \sim N^{-\gamma_z} \quad (13)$$

In Fig. 9, γ_{xy} is 4.77, 3.90, and 3.32, respectively for protein-like chains with adsorption energy $\epsilon_{\text{ads}} = 0, -6, \text{ and } -9$. However, γ_z is 4.68, 5.60, and 5.74 respectively for protein-like chains with adsorption energy $\epsilon_{\text{ads}} = 0, -6, \text{ and } -9$. Here we find that the values of γ_{xy} and γ_z are almost equal for protein-like chains without adsorption energy, and γ_{xy} decreases, while γ_z increases when adsorption energy becomes strong.

In Fig. 9, we also give the results for SAW chain without adsorption interaction energy, and the values of γ_{xy} and γ_z are 1.02 and 1.01, respectively. Therefore, we find that dynamics of adsorbed protein-like chains are completely different from general polymer chains, and these investigations can provide some insights into the adsorption of proteins.

4. Conclusions

Conformations and dynamics of adsorbed protein-like chains are investigated by using Monte Carlo simulation method based on the modified orientation-dependent monomer–monomer interactions (ODI) model. In our modified ODI model, the secondary structure of proteins of α -helical and β -sheet can be considered simultaneously.

At the same time, comparisons with SAW chains are also made.

Chain size and shape of adsorbed protein-like chains are investigated by calculating mean-square end-to-end distance $\langle R^2 \rangle$, mean-square radius of gyration $\langle S^2 \rangle_{xy}$ (or $\langle S^2 \rangle_z$), shape factors $\langle sf_i^* \rangle$ ($i = 1, 2, 3$), and $\langle \delta^* \rangle$. Some different results from general polymer chains are obtained in the chain size and shape of adsorbed protein-like chains. In the meantime, from the results of $\langle sf_i^* \rangle$ and $\langle \delta^* \rangle$, we can find that protein-like chains without adsorption interaction energy have globular structures, and the shape becomes flat when adsorption interaction energy becomes strong. Some discussions about fraction of adsorbed segment f_a and average orientation of bond $\langle P_2(\cos \theta) \rangle$ are also presented.

We investigate dynamics of protein-like chains by calculating the diffusion coefficients D with different adsorption interaction energy. Some important results are obtained here. There exist relationships between the diffusion coefficients and chain length N , i.e. $D_{xy} \sim N^{-\gamma_{xy}}$ and $D_z \sim N^{-\gamma}$. However, the values of γ_{xy} and γ_z are 4–5 times larger than that of SAW chains. These results can help us understand the adsorption of proteins in more detail.

This paper mainly discusses the conformations and dynamics of adsorbed protein-like chains, therefore, we investigate the effect of adsorptions on these properties through considering different adsorption energies. In the future, we will consider different secondary structures of adsorbed protein-like chains and explore the influences of secondary structures to the conformations and dynamics of protein-like chains. In the meantime, we will also investigate the effects of secondary structure on the elastic behaviors of adsorbed protein-like chains.

Acknowledgements

This research was financially supported by National Natural Science Foundation of China (Nos. 20174036, 20274040), and Natural Science Foundation of Zhejiang Province (Nos. R404047). We also thank the referees for their critical reading of the manuscript and their good ideas.

References

- [1] Imbert-Laurenceau E, Berger MC, Pavon-Djavid G, Jouan A, Véronique M. *Polymer* 2005;46:1277–85.
- [2] Laguecir A, Stoll S. *Polymer* 2005;46:1359–72.
- [3] Be'al L, Chevalier Y. *Polymer* 2005;46:1395–405.
- [4] Hermesen GF, Wessling M, Van der Vegt NFA. *Polymer* 2004;45:3027–36.
- [5] Munro JC, Frank CW. *Polymer* 2003;44:6335–44.
- [6] Miyazaki T, Shimazu A, Ikeda K, Kanaya T. *Polymer* 2003;44:1553–9.
- [7] Hu TJ, Gao J, Auweter H, Iden R, Lueddecke E, Wu C. *Polymer* 2002;43:5545–50.
- [8] Abraham T. *Polymer* 2002;43:849–55.
- [9] Kasemo B. *Curr Opin Solid State Mater Sci* 1998;3:451–9.
- [10] Brash JL, Horbett TA. In: Horbett TA, Brash JL, editors. *Proteins at interfaces II*. Washington, DC: ACS; 1995.
- [11] Verdier PH, Stockmayer VH. *J Chem Phys* 1966;45:2122–8.
- [12] Madras N, Sokal AD. *J State Phys* 1988;50:109–86.
- [13] Deutsch HP, Binder K. *J Chem Phys* 1991;94:2294–304.
- [14] Wang Y, Rajagopalan R. *J Chem Phys* 1996;105:696–705.
- [15] Chen J, Zhang LX, Cheng J. *J Chem Phys* 2004;121:11481–8.
- [16] Zhdanov VP, Kasemo B. *Proteins: Struct, Funct, Genet* 2000;39:76–81.
- [17] Zhdanov VP, Kasemo B. *Proteins: Struct, Funct, Genet* 1998;30:168–76.
- [18] Zhdanov VP, Kasemo B. *Proteins: Struct, Funct, Genet* 1998;30:177–82.
- [19] Zhdanov VP, Kasemo B. *Phys Rev E* 1997;56:2306–9.
- [20] Zhdanov VP, Kasemo B. *Proteins: Struct, Funct, Genet* 2000;40:539–42.
- [21] Chen J, Zhang LX. *Colloids Surf, A: Physiochem Eng Asp*. 2005. In press.
- [22] Zhang LX, Chen J. *Polymer*. 2005. In press.
- [23] Zhdanov VP, Kasemo B. *Proteins: Struct, Funct, Genet* 1997;29:508–16.
- [24] Sun TT, Zhang LX. *Polymer* 2004;45:7759–66.
- [25] Verdier PH, Stockmayer WH. *J Chem Phys* 1962;36:227–35.
- [26] Hilhorst HJ, Deutch JM. *J Chem Phys* 1975;63:5153–61.
- [27] Solc K, Stockmayer WH. *J Chem Phys* 1971;54:2981–8.
- [28] Solc K. *J Chem Phys* 1971;54:2756–7.
- [29] Mazur J, Guttman GM, McCrackin FL. *Macromolecules* 1973;6:872–4.
- [30] Jagodzinski O, Eisenriegler E, Kremer K. *J Phys I* 1992;2:2243–79.
- [31] Diehl HW, Eisenriegler E. *J Phys A: Math Gen* 1989;22:L87–L91.
- [32] Rudnick J, Gaspari G. *J Phys A* 1986;19:L191–L3.
- [33] Wei G. *Macromolecules* 1997;30:2130–4.
- [34] Teraoka I. *Polymer solutions*. New York: Wiley; 2002.
- [35] Nienhuis B. *Phys Rev Lett* 1982;49:1062–5.